

## Topographical Variation in Metabolic Signatures of Human Gastrointestinal Biopsies Revealed by High-Resolution Magic-Angle Spinning $^1\text{H}$ NMR Spectroscopy

Yulan Wang,<sup>†</sup> Elaine Holmes,<sup>†</sup> Elena M. Comelli,<sup>‡</sup> Grigorios Fotopoulos,<sup>‡</sup> Gian Dorta,<sup>#</sup>  
Huiru Tang,<sup>§</sup> Mattias J. Rantalainen,<sup>†</sup> John C. Lindon,<sup>†</sup> Irène E. Corthésy-Theulaz,<sup>‡</sup>  
Laurent B. Fay,<sup>‡</sup> Sunil Kochhar,<sup>‡</sup> and Jeremy K. Nicholson<sup>\*,†</sup>

*Department of Biomolecular Medicine, SORA Division, Faculty of Medicine, Imperial College London, Sir Alexander Fleming Building, South Kensington, London SW7 2AZ, United Kingdom, Department of Nutrition and Health and Bioanalytical Sciences, Nestlé Research Center, P.O. Box 44, Vers-chez-les-Blanc, CH-1000 Lausanne 26, Switzerland, State Key Laboratory of Magnetic Resonance and Atomic and Molecular Physics, Wuhan centre for Magnetic Resonance, Wuhan Institute of Physics and Mathematics, The Chinese Academy of Sciences, Wuhan, 430071, PR China, and Department of Gastroenterology, BH 10/535, CHUV, CH-1011 Lausanne, Switzerland*

Received May 3, 2007

Individual and topographical variation in the metabolic profiles of multiple human gastrointestinal tract (GIT) biopsies have been characterized using high-resolution magic-angle spinning (HRMAS)  $^1\text{H}$  NMR spectroscopy and pattern recognition. Samples from antrum, duodenum, jejunum, ileum, and transverse colon were obtained from 8 male and 8 female participants. Each gut region generated a highly characteristic metabolic profile consistent with the varying structural and functional properties of the tissue at different longitudinal levels of the gut. The antral (stomach) mucosa contained higher levels of choline, glycogen, phosphorylethanolamine, and taurine than other gut regions. The spatially close regions of the duodenum and jejunum were equivalent in terms of their gross biochemical composition with high levels of choline, glutathione, glycerophosphocholine (GPC), and lipids relative to other gut regions. The ileal mucosa showed poor discrimination from the duodenum and jejunum tissues and generated strong amino acids signatures but had relative low GPC signals. The colon (large intestine) was high in acetate, glutamate, inositols, and lactate and low in creatine, GPC, and taurine compared to the small intestine. These longitudinal metabolic variations in the human GIT could be attributed to functional variations in energy metabolism, osmoregulation, gut microbial activity, and oxidative protection. This work indicates that  $^1\text{H}$  HRMAS NMR studies may be of value in analyzing local metabolic variation due to pathological processes in gut biopsies.

**Keywords:** metabonomics • antrum • duodenum • jejunum • ileum • intestine • human • pattern recognition • biopsy • magic-angle spinning NMR spectroscopy

### Introduction

The gastrointestinal tract (GIT) is a primary interface between an animal and its environment, and apart from its obvious critical role in digestive and nutrient absorption, it is the site of interaction and entry of many pathogens and toxins. The GIT is highly functionally specialized and longitudinally stratified, with epithelial cell types, secretions, and generalized anatomical wall structure varying accordingly.<sup>1</sup> Many human diseases are related to dysfunction of the gut itself or are associated with a variety of gut disorders. Moreover, the

complex associations between nutrition and gut activity impact strongly upon the development of potentially morbid conditions such as obesity.<sup>2</sup> Hence, understanding variation in gut biochemistry in man may be of crucial importance with respect to the understanding of the molecular etiology underpinning many human diseases.<sup>3–6</sup> Furthermore, the gut houses a complex and flexible consortium of microbes (the microbiome) present at extraordinarily high population densities conferring a myriad of advanced digestive, metabolic, and immunological properties on the host.<sup>7,8</sup> These microbes exert a profound effect on the development, structure, and digestive and absorptive capabilities of the intestinal epithelium.<sup>9–11</sup> The microbiota also influence the activity of the enteric nervous system, aid the extraction and processing of nutrients from otherwise indigestible food,<sup>12</sup> and may have long-range endocrine-regulatory functions *via* their co-metabolic effects on bile acid composi-

\* To whom correspondence should be addressed. E-mail: j.nicholson@imperial.ac.uk.

<sup>†</sup> Imperial College London.

<sup>‡</sup> Nestlé Research Center.

<sup>§</sup> The Chinese Academy of Sciences.

<sup>#</sup> Department of Gastroenterology, BH 10/535.

tion.<sup>13</sup> Understanding the relationships between the molecular features and the biological function of structurally and functionally distinct regions of the GIT in a holistic manner is important in knowing the state of health and in understanding metabolic deviations associated with disease, diet, and environment.

High-resolution magic-angle spinning (HRMAS) <sup>1</sup>H NMR spectroscopy of intact tissue samples is a powerful tool for the non-destructive measurement of metabolic fingerprints in small samples of biological tissues.<sup>14</sup> We have previously shown that this approach can be a valuable addition to high-resolution NMR spectroscopic studies on biofluids for understanding disease profiles, which are caused by experimental pathogens or by other means, especially when combined with pattern recognition methods.<sup>15–18</sup> In addition, HRMAS NMR spectroscopy has been applied to the characterization of intact rat liver,<sup>19–21</sup> heart,<sup>22</sup> kidney,<sup>23,24</sup> testis,<sup>25</sup> human breast,<sup>26</sup> and prostate<sup>27</sup> in healthy and diseased animals and humans. HRMAS NMR spectroscopy has also been employed to study the biochemistry of healthy human gastric mucosa, where more than 40 metabolites have been identified.<sup>28</sup> A recent study using this technique to characterize the metabolic composition of rat jejunum and ileum showed that the jejunum was rich in lipids and triglycerides which is consistent with its role in fat storage, whereas the ileum was more abundant in amino acids.<sup>29</sup> In addition, metabolic profiles of intestinal regions have been found to vary with age; for example, the relative levels of lipids, lactate, taurine, and creatinine were found to increase with age, while the relative levels of amino acids and glycerophosphocholine (GPC) were decreased in older animals.<sup>29</sup> Here, we extend these studies to characterize systematically the biochemical composition of a comprehensive range of intact human intestinal biopsies from healthy men and women. We apply <sup>1</sup>H HRMAS NMR spectroscopy in combination with orthogonal projection to latent structure-discriminant analysis (O-PLS-DA) to metabolically profile samples from antrum, duodenum, jejunum, ileum, and transverse colon with the aim of providing baseline data that will be of value when assessing disturbed metabolic profiles in biopsies from diseased patients.

## Experimental Methods

**Sample Collection.** The study protocol was approved by the Ethical Committee of the Etat de Vaud, Lausanne, Switzerland. Twenty healthy men ( $n = 10$ ) and women ( $n = 10$ ) aged between 20 and 30 years were enrolled in the study, and written consent was obtained from each participant. The recruitment was conducted according to the Helsinki declaration. A health check on the participants was carried out prior to sampling to ensure that they were free from certain diseases including neoplastic, cardiovascular, hepatic, renal, or inflammatory bowel diseases. In addition, blood tests were carried out including assessment of *Helicobacter pylori* absence and normal coagulation markers (thromboplastin time, TP > 70%, platelets > 150 000/mm<sup>3</sup>, partial thromboplastin time, pTT, normal), and it was established that participants were not hemophilic. The participants had not been taking any drugs or anti-coagulative treatment during the 4 weeks before sampling. All participants were required to fast for 12 h and took a routinely used bowel preparation on the evening before the procedure, which consisted of 4 L of Fordtran solution and 3 L of Cololyt. Biopsy samples from the antrum, duodenum, jejunum, ileum, and transverse colon of these participants were collected at the Gastroenterology Department of the Hospital University Centre

in Canton de Vaud, Lausanne, Switzerland by endoscopy or colonoscopy under sedation (Dormicum 2.5–5 mg IV and/or Pethidine 25–50 mg IV). Since the size of a biopsy is small (~10–15 mg), it can be assumed that mainly the mucosa was sampled. Biopsies from 16 participants (8 males and 8 females) were snap-frozen immediately after collection and stored at –80 °C for NMR analysis, and the biopsies from the remaining volunteers were frozen in RNA lysis solution for gene expression analysis which will be reported separately.

**<sup>1</sup>H HRMAS NMR Spectroscopy.** Samples of human biopsies (~10–15 mg) were packed individually into 4 mm diameter zirconia rotors and closed with a spherical insert and Kel-F cap. A drop of D<sub>2</sub>O was added into the rotor to provide a field lock for the NMR spectrometer. All NMR experiments were carried out on a Bruker DRX-600 spectrometer (Bruker Biospin, Rheinstetten, Germany), operating at a <sup>1</sup>H frequency of 600.11 MHz and equipped with a triple-resonance, high-resolution, magic-angle spinning (MAS) probe with a magic-angle gradient. Samples were spun at 5 kHz at the magic angle (54.7°) and maintained at 283 K in order to minimize degradation of tissues.<sup>30</sup> A total of 15 min was allowed for the temperature to reach equilibration for each sample before a spectrum was acquired. The 90° pulse length (~9.0 μs) was adjusted individually for each sample. A total of 128 transients were collected into 16 k data points for each spectrum with a spectral width of 20 ppm and a recycle delay (RD) of 2.0 s.

Three <sup>1</sup>H NMR spectra were acquired for each sample: (1) A standard one-dimensional NMR spectrum which is a general representation of the total biochemical composition, was acquired using the first increment of the noesy pulse sequence to achieve water presaturation [90- $t_1$ -90- $t_m$ -90-acq].<sup>31</sup> (2) A Carr-Purcell-Meiboom-Gill (CPMG) spin-echo pulse experiment used to attenuate interfering signals from macromolecules with short spin-spin relaxation times was acquired using the CPMG pulse sequence [90-( $T$ -180- $T$ ) $_n$ -acq].<sup>32</sup> (3) A diffusion-edited NMR spectrum which selectively measures large macromolecules was acquired using the bipolar-pair longitudinal-eddy-current (BPP-LED) pulse sequence [RD-90°- $G_1$ - $\tau$ -180°- $G_2$ - $\tau$ -90°- $\Delta$ -90°- $G_3$ - $\tau$ -180°- $G_4$ - $\tau$ -90°- $T_e$ -90°-acq].<sup>33</sup> For the standard one-dimensional experiment, the inter-pulse delay  $t_1$  was 3 μs, the mixing time  $t_m$  was 100 ms, and irradiation of the water resonance was used during  $t_m$  and RD. For the CPMG experiment, water peak presaturation and a spin-spin relaxation delay,  $2n\tau$ , of 200 ms was used for all samples. A sine-shaped gradient strength  $G$  15.8 G/cm and duration of 2.5 ms was used for diffusion-edited spectra, followed by a delay ( $\tau$ ) of 400 μs to allow for the decay of eddy currents. A diffusion time ( $\Delta$ ) of 100 ms and a delay  $T_e$  of 5 ms were used together with water peak irradiation during RD. For assignment purposes, two-dimensional (2D) <sup>1</sup>H-<sup>1</sup>H Correlation Spectroscopy (COSY)<sup>34</sup> and Total Correlation Spectroscopy (TOCSY)<sup>35</sup> NMR spectra were also acquired for selected intestinal samples as detailed previously.<sup>29</sup>

**Data Analysis.** Free induction decays were multiplied by an exponential function equivalent to a 0.3 Hz line-broadening factor prior to Fourier transformation and were corrected for phase and baseline distortions using XWINNMR 3.5 (Bruker). The spectra were referenced to the chemical shift of the peak of the anomeric proton of  $\alpha$ -glucose at  $\delta$  5.223. The spectra over the range  $\delta$  0.5–10.0 were digitized using a Matlab script developed in-house at Imperial College London (Dr. O. Cloarec). The region  $\delta$  4.66–5.20 was removed to avoid the effects of imperfect water suppression. The region  $\delta$  3.62–3.75 was also

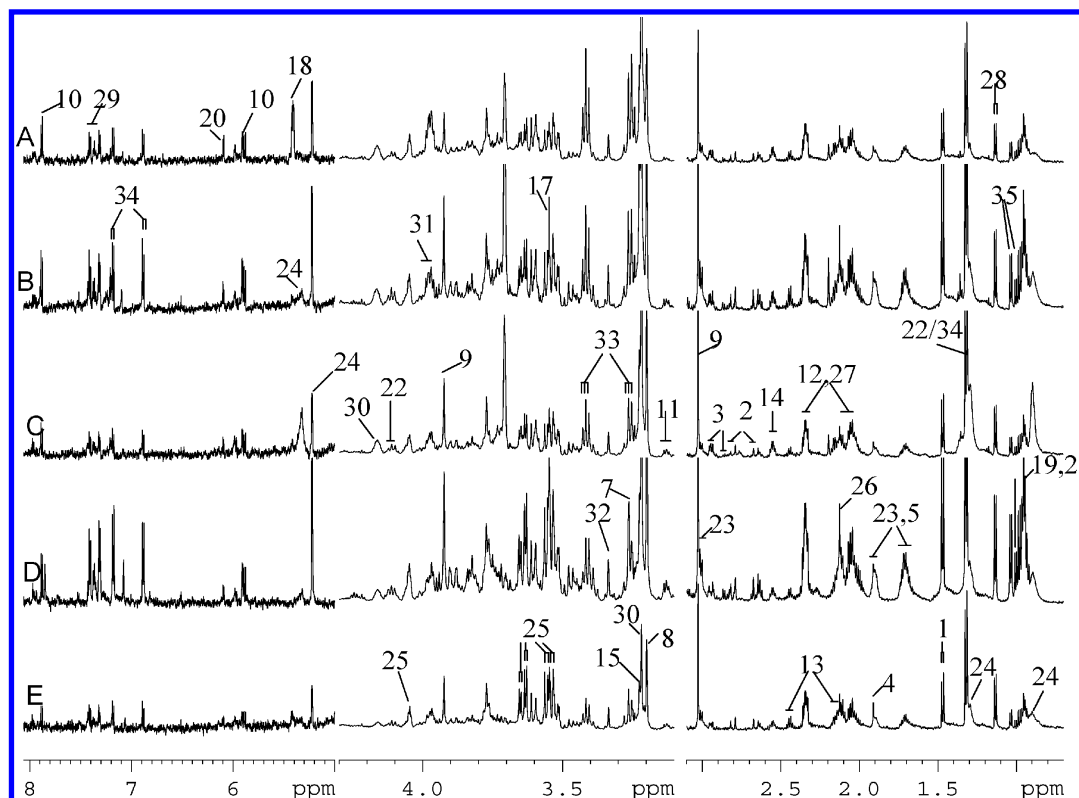


**Figure 1.** 600 MHz  $^1\text{H}$  HRMAS CPMG NMR spectra of human biopsies obtained from antrum (A), duodenum (B), jejunum (C), ileum (D), and transverse colon (E). The region between  $\delta$  5.0–8.0 was magnified 8 times, and the region  $\delta$  0.7–3.1 was magnified 4 times compared with the region  $\delta$  3.0–4.3 for the purpose of clarity. Keys: 1, alanine; 2, aspartic acid; 3, asparagine; 4, acetate; 5, arginine; 6, *N*-acetyl glycoproteins; 7, betaine; 8, choline; 9, creatine; 10, cytosine; 11, ethanolamine; 12, glutamate; 13, glutamine; 14, glutathione; 15, GPC; 16,  $\alpha$ -glucose; 17, glycine; 18, glycogen; 19, isoleucine; 20, isocytosine; 21, leucine; 22, lactate; 23, lysine; 24, lipid; 25, *myo*-inositol; 26, methionine; 27, proline; 28, propylene glycol; 29, phenylalanine; 30, phosphorylcholine; 31, phosphorylethanolamine; 32, *scyllo*-inositol; 33, taurine; 34, tyrosine; 35, valine.

removed due to the presence of peaks from an exogenous compound used in the bowel preparation. Normalization to the sum of the spectrum was carried out on the data prior to pattern recognition analyzes. Discriminant analysis using the O-PLS<sup>36</sup> algorithm was carried out on the NMR spectra; data were mean-centered and scaled to unit variance prior to analysis. O-PLS is an extension of the Partial Least-Square regression method<sup>37</sup> featuring an integrated Orthogonal Signal Correction filter.<sup>38</sup> For visualization purposes, the O-PLS coefficients indicating those variables contributing to the discrimination in the model were back-transformed as described by Cloarec et al.<sup>39</sup> All data analysis was carried out using MATLAB 7.0 with scripts developed in-house at Imperial College London. The validation of the model was conducted using 7-fold cross validation, that is, iterative construction of models by repeatedly leaving out one-seventh of the samples, and predicting them back into the model. The classification accuracy of the O-PLS-DA model was established from the prediction-set samples in the 7-fold cross-validation, using a decision-rule based on the largest predicted *Y* value. Classification performance was evaluated, by *sensitivity* and *specificity* levels. Sensitivity is defined as the true positive ratio (i.e., number of true positives/(number of true positives + number of false negatives)), and specificity is defined as the true negative ratio (i.e., number of true negatives/(number of true negatives + number of false positives)). An additional confusion matrix was established to allow for the assessment of how misclassified samples were classified by the O-PLS-DA model. In addition,

the statistical total correlation spectroscopy (STOCSY)<sup>40</sup> method was also applied in order to correlate NMR resonances of selected NMR signals as an aid to metabolite assignment.

## Results

**$^1\text{H}$  HRMAS NMR Spectra of Human Gastrointestinal Mucosa.** Typical  $^1\text{H}$  CPMG HRMAS NMR spectra of intact human biopsies of the antrum, duodenum, jejunum, ileum, and transverse colon obtained from a female participant are shown in Figure 1. In total, 35 common metabolites were identified including a range of amino acids, carboxylic acids, pyrimidines, and membrane component metabolites, as well as creatine, glucose, inositols, lipids, and triglycerides. The NMR resonance assignments were taken from literature and confirmed using two-dimensional NMR spectra.<sup>28,29</sup> The assignment of betaine was confirmed using STOCSY analysis which showed high correlation between the singlet at  $\delta$  3.26 and the singlet at  $\delta$  3.91. The global biochemical composition of various human GIT samples was similar irrespective of the position along the intestine, but variation in the relative signal intensities could be associated with specific topographical locations. For example, ileal mucosa appeared to be rich in amino acids, whereas a relative lower level of taurine was present in mucosa of the transverse colon. To systematically investigate the relative intensities of specific metabolites associated with each part of the intestinal mucosa, O-PLS-DA<sup>36,39</sup> was applied to these NMR spectral data acquired for each region. Multivariate modeling

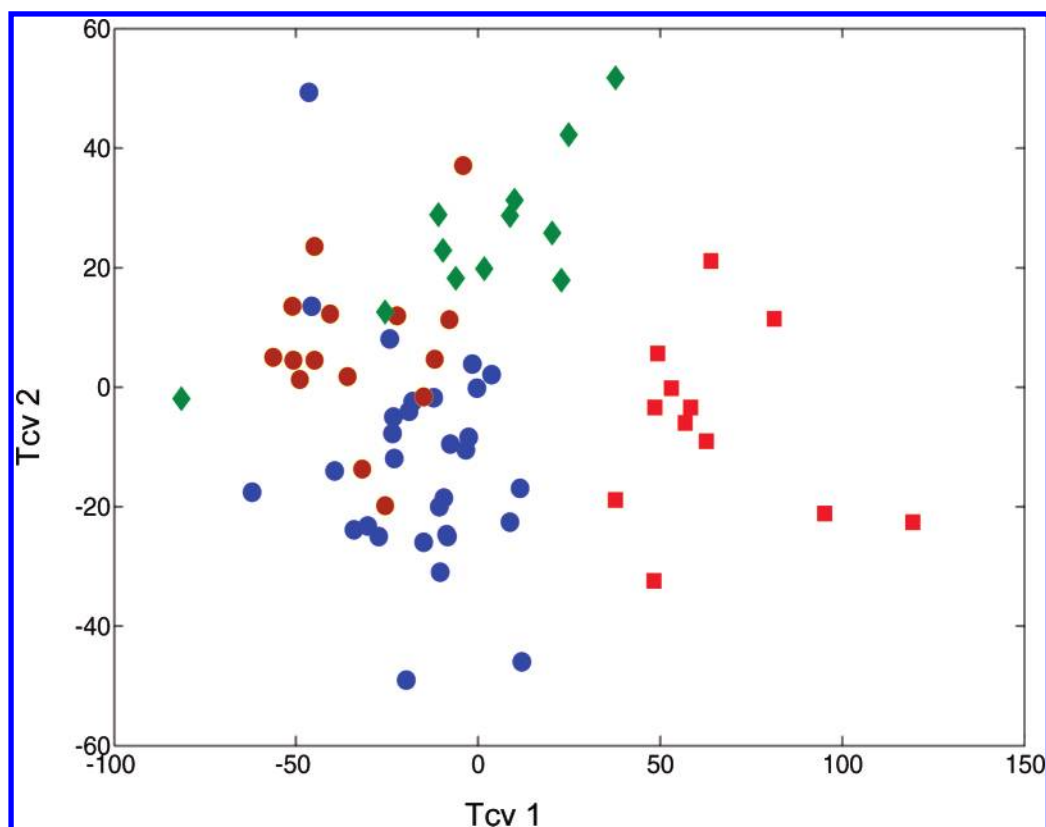


**Figure 2.** O-PLS-DA cross-validated scores plot showing differentiation of the metabolic profiles of localized gastrointestinal compartments. Red, antrum; blue, combined duodenum and jejunum; brown, ileum; green, colon.

of both the standard one-dimensional NMR spectral data and the CPMG spectral data sets showed good discrimination of mucosa types, but the diffusion-edited spectral data set did not show such regional dependent variation. This indicates that the lipoprotein/lipid profile was relatively consistent across the sample types with the major variation being in the low molecular weight metabolites. Therefore, only results from the CPMG spectra data set are presented here to avoid unnecessary duplication.

**O-PLS-DA of NMR Spectra of Human Gastrointestinal Mucosa.** No gender variation was observed in the current study for any part of the gastrointestinal mucosa using O-PLS-DA modeling of unit variance scaled CPMG spectral data. Each tissue region was compared with every other region in a series of pairwise comparisons. The results suggested that the variations in biological composition between duodenum and jejunum were negligible. Therefore, NMR data of mucosa samples from duodenum and jejunum were combined and considered as one group in subsequent analyses. An O-PLS-DA model was constructed using NMR data as an **X** matrix and class information as the **Y** variables,<sup>39</sup> that is, antrum (class 1), ileum (class 2), duodenum and jejunum (class 3), and transverse colon (class 4). Two **Y** orthogonal components and three predictive O-PLS components were calculated for the model. The total explained variation for the **X** matrix was 0.3 ( $R^2X$ ), and the corresponding cross-validation parameter ( $Q^2Y$ ) indicating the predictability of the model was 0.39. The cross-validated scores plot showed good separation of the antrum samples in the first component with differentiation of the colon and combined duodenum and jejunum in the second component. Samples from ileum overlapped partially with the samples from both colon and the duodenum/jejunum (Figure 2). Table 1 illustrates

**Table 1.** Confusion Matrix Calculated from O-PLS-DA Model Indicating the Classification Results for Each Class<sup>a</sup>

true class	predicted class			
	antrum	ileum	duodenum/jejunum	colon
Antrum	0.78	0	0.22	0
Ileum	0	0.40	0.50	0.10
Duodenum/Jejunum	0	0.10	0.90	0
Colon	0	0.10	0.10	0.80

<sup>a</sup> Values indicate the ratio between predicted samples and the total number of samples in each intestinal segment class (row).

the sensitivity and specificity levels for each class in this O-PLS-DA model, confirming the observation in the scores plot indicating that the antrum was the best metabolically characterized region, showing both high sensitivity (78%) and specificity (100%) levels. However, while the ileum showed low sensitivity (40%), the confusion matrix (Table 1) indicates that this is due to the ileum being poorly distinguished from duodenum/jejunum (50% ileal samples were misclassified as duodenum/jejunum). Some overlap of structure/function may be expected between adjacent small intestinal segments.

O-PLS-DA coefficient plots illustrating the various metabolites associated with a specific intestinal mucosa as compared to mucosa obtained from all other regions of the intestine are shown in Figure 3. The coefficient plot displays the differences in metabolic profiles related to class or sample type. Here, the direction of the resonances relates to the relative intensity of metabolites in a class of interest with respect to the remaining classes as calculated from the covariance matrix. Thus positive peaks in Figure 3A, for example, indicate a relatively higher intensity of metabolites associated with antrum in comparison



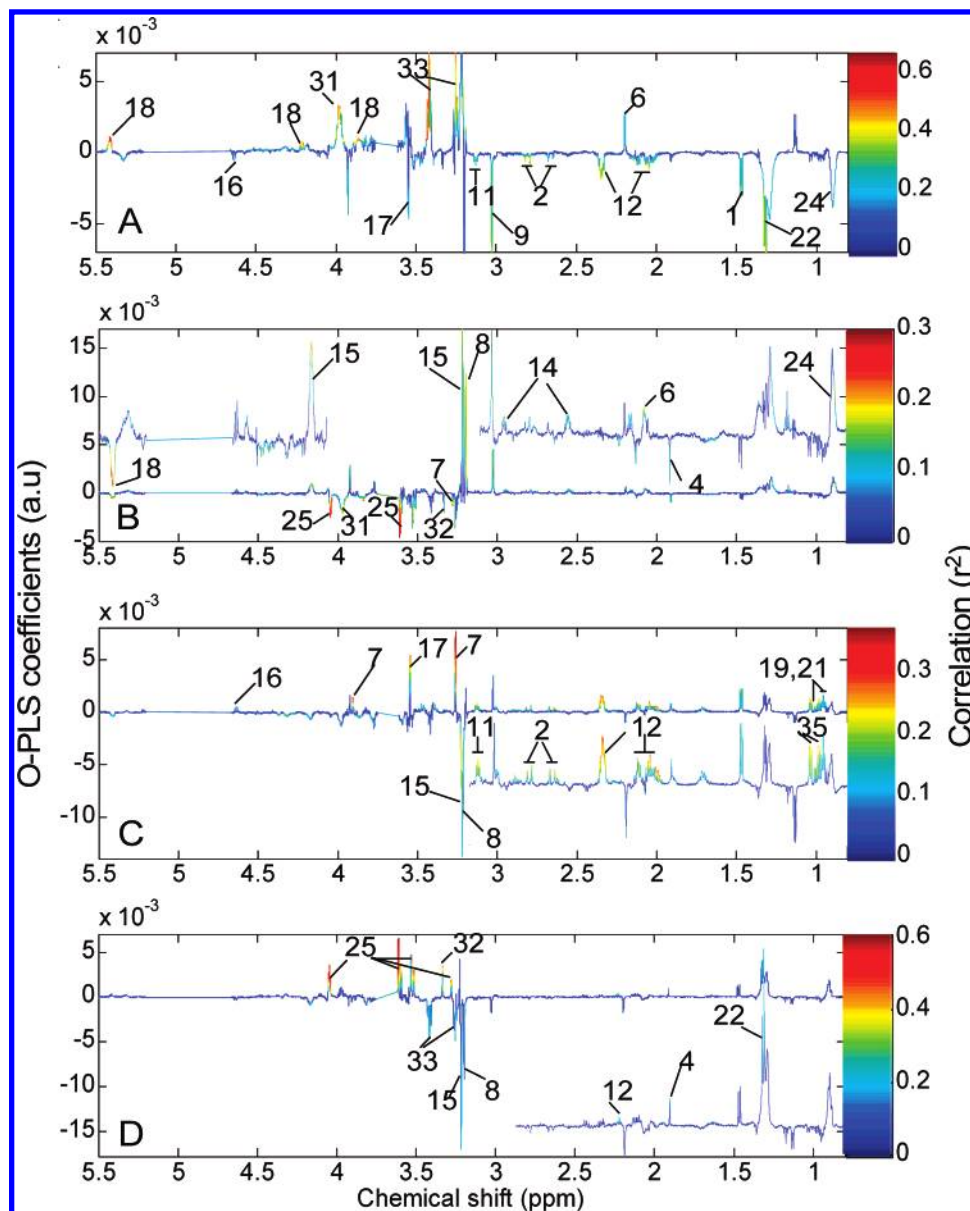


**Figure 3.** O-PLS-DA coefficient plots corresponding to the characterization of antrum (A), duodenum/jejunum (B), ileum (C), and transverse colon (D). The colors shown on the plot are associated with the significance of metabolites in characterizing the NMR data for the class of interest with the scale shown on the right-hand side of each coefficient plot.

to all other regions. The colors shown on the plot are associated with the significance of metabolites in characterizing the NMR data for the class of interest and are calculated using the correlation matrix with the scale shown on the right-hand side of each plot. The coefficients indicating the significance of the metabolites correlated with mucosa obtained from different compartments of human GIT are summarized in Table 2. Here, the coefficient is considered to be significant when higher than 0.35, which corresponds to the critical value of a correlation coefficient of 5% ( $p = 0.05$ ) for a given data point. These data show that the antrum contained relative higher levels of choline, glycogen, phosphorylethanolamine, taurine, and acetyl glycoproteins than the other regions considered. These variations were associated with relatively lower levels of amino acids, lipids, glucose, and lactate in the antrum. The duodenum and jejunum were similar in terms of their biochemical composition and were rich in choline, glutathione, GPC, lipids, and glycoproteins but contained relatively lower levels of acetate, betaine,

glycogen, inositols, and phosphorylethanolamine in comparison with other intestinal regions. In contrast to the other regions, especially the antrum, the ileum was rich in amino acids, but low in GPC. The metabolites exerting the greatest influence on the separation of transverse colonic mucosa from the other intestinal regions were acetate, glutamate, inositols, lactate, which were all present in relatively high levels, and creatine, GPC, and taurine, which were present in relatively lower amount (Table 2).

## Discussion

Each topographically distinct portion of the intestine was characterized by its metabolic profile with closer metabolic similarities generally observed between adjacent sections, such as high similarity between ileum and the jejunum and duodenum (Table 1) and clear boundaries observed between small intestine and colon (Figure 2). This observation is consistent

**Table 2.** The Coefficients of Metabolites in the CPMG Spectra Contributing to the Separation of a Specific Human Gastrointestinal Region from All the Others ( $R^2Y = 0.84$ ,  $R^2X = 0.30$ ,  $Q^2Y = 0.39$ )<sup>a</sup>

metabolites ( $\delta$ ppm)	duodenum			
	antrum	jejunum	ileum	colon
alanine (1.46)	-0.49			
acetate (1.91)		-0.35		+0.35
aspartic acid (2.78)	-0.57		+0.50	
betaine (3.26)		-0.40	+0.59	
choline (3.19)	+0.69	+0.40	-0.35	-0.36
creatine (3.03)	-0.55	+0.32		
ethanolamine (3.13)	-0.46		+0.46	
glutamate (2.34)	-0.61		+0.52	+0.48
glycine (3.55)	-0.44		+0.51	
glycogen (5.41)	+0.77	-0.40		
glutathione (2.55)		+0.37		
glucose (4.63)	-0.40			
GPC (3.23)		+0.38	-0.45	-0.38
leucine/isoleucine (1.00)			+0.44	
lipids (5.32)	-0.36	+0.36		
lactate (1.33)	-0.55			+0.40
<i>myo</i> -inositol (4.04)		-0.53		+0.75
<i>N</i> -acetyl glycoproteins (2.07)	+0.39	+0.40	+0.35	
phosphorylethanolamine (3.98)	+0.69	-0.38		
scyllo-inositol (3.34)		-0.37		+0.61
taurine (3.25)	+0.69			-0.40
valine (1.04)			+0.48	

<sup>a</sup> The + and - symbols indicate the presence of higher (+) or lower (-) levels of metabolite with respect to the levels found in other intestinal tissues.

the results obtained from gene expression profiles of the GIT of adult mouse.<sup>41</sup>

Relatively higher levels of phospholipids intermediates including choline, phosphorylethanolamine (PE), and GPC were mainly associated with upper parts of the human GIT. Choline is an important compound for mammals, as it is a precursor for biosynthesis of phospholipids that are essential constituents of all membranes. Previous investigations have reported a relatively high level of GPC in the duodenum and jejunum,<sup>29</sup> which is consistent with the data presented here and may be explained by the functional role of these regions in the intestinal absorption of dietary phospholipids. It has been suggested that dietary phospholipids are hydrolyzed in the intestinal lumen by pancreatic phospholipase-A to monoacylglycerol, which on entering the epithelial cells is hydrolyzed again by esterase and release fatty acids while the rest is further hydrolyzed to GPC.<sup>42</sup>

Variation in the relative level of amino acids was a dominant aspect of differentiation between human GIT regions. For example, relatively higher levels of aspartate, glutamate, glycine, leucine, isoleucine, and valine were found in the ileum compared to other parts of intestine. This observation in man is consistent with a previous investigation of rat intestine composition.<sup>29</sup> Amino acids are required by cells of the small intestinal mucosa for protein and for energy generation.<sup>43,44</sup> For example, glutamine is an important fuel for the mucosal cells of the small intestine and has a key role in maintaining the function and integrity of the intestine.<sup>43</sup> Other amino acids, particularly glutamate and aspartate, are also catabolized as fuel.<sup>45</sup>

The colon was characterized by a relatively high level of lactate. It has been shown that the enzyme activities involved in glycolysis along the small intestine of the rat, including hexokinase and 6-phosphofructokinase, are decreased by 50%, whereas glucose 6-phosphatase is decreased by an order of

magnitude from duodenum to caecum.<sup>46</sup> The fact that the activity of hexokinase is considerably greater than that of glucose 6-phosphatase in the lower part of the intestine may result in some of the glucose being metabolized to lactate,<sup>46</sup> which is consistent with elevated lactate levels observed in human mucosal of the colon. The possibility of lactate produced from anaerobic glycolysis during NMR acquisition can be ruled out, since previous investigation has shown no change in terms of the biochemical composition being observed for liver standing on ice for 5 h.<sup>30</sup>

Acetate was also found in high level in colon biopsies when compared to other parts of the intestine. Acetate is produced from fibers fermentation by the gut microbiota.<sup>47</sup> The microbial population density increases distally along the GIT, and it is highest in the colon,<sup>48,49</sup> which is consistent with the observation of higher level of acetate in mucosa of the human colon.

Intestinal epithelial cells are subjected to hypertonic conditions when digested foods enter the GIT. Therefore, osmotic regulation is important in the GIT for balancing the osmotic equilibrium between the cell and its surrounding medium. Such regulation is achieved through maintaining a high intracellular content of osmolytes such as betaine, *myo*-inositol, *scyllo*-inositol, and taurine.<sup>50</sup> It is interesting to note that, although the above-mentioned organic osmolytes were present in all intestinal regions, variations in terms of their relative intensities were associated with specific parts of the human GIT. For example, the relative level of betaine was found to be the highest in the ileal mucosa, whereas that of taurine was the highest in the antrum. The transverse colon was rich in *myo*-inositol and *scyllo*-inositol. Accumulation of betaine has been found in the intestine of hamsters,<sup>51</sup> rabbits,<sup>52</sup> and broiler chicks.<sup>53,54</sup> *Myo*-inositol and its various biochemical derivatives are broadly distributed in mammalian organs and cells, such as in the brain, testis, secretory tissues, and kidney. Recently, the cDNA encoding for *myo*-inositol 1-phosphate synthase, an important enzyme for controlling the concentration of *myo*-inositol, has been cloned from human colon.<sup>55</sup> Taurine is another commonly found osmolyte in animal organs such as the kidney. Specific roles for taurine in maintaining cell volume under short-term hypo-osmotic stress, and inositol for long-term hypo-osmotic/hyper-osmotic stress, have been reported.<sup>56</sup> The different functions of these two organic osmolytes could be related to the localization of the organic osmolytes at specific intestinal mucosa, that is, association of taurine with antrum and inositols with colon, and hence to the physiological state.

The human GIT is also subjected to oxidative stress, especially from free radicals generated from lipid metabolism. Distribution of glutathione, one of the most important anti-carcinogens and antioxidants in mammalian cells,<sup>57</sup> was found throughout the human intestine with its level being relatively high in the mucosa of duodenum and jejunum. This observation is consistent with previous studies in both humans<sup>58,59</sup> and rats.<sup>57</sup> Additional glutathione could also arise from the release of bile from the bile duct which is connected to the duodenum and jejunum.<sup>57</sup> We have also observed a relative decreased level of glutathione in the ileum and colon. This could be associated with increased microbial population density in these regions compared to more proximal intestinal segments, since it has been suggested that microbiota toxins production may be related to glutathione levels.<sup>60</sup>

The human GIT is prone to mechanical and chemical stress. In the current investigation, higher levels of acetyl glycoproteins were found in the antrum and duodenum when compared to

the other parts of the GIT. The results obtained here are also consistent with the recent discovery of a high level of synaptophysin, a glycoprotein found in the antrum of the human GIT.<sup>61</sup> Glycoproteins are high molecular weight polymers and important constituents of mucins.<sup>44,62</sup> The functions of mucins are tissue lubrication and modulation of water and electrolyte absorption, and most importantly, they provide protection of the epithelium from mechanical and chemical stress.<sup>63</sup> The observation of high levels of glycoproteins in antrum and duodenum could be anticipated, since the mucosal lining of the antrum and duodenum is exposed to high levels of hydrochloric acid and pepsin, essential for protein digestion. This therefore requires mucin-secreting cells to produce a healthy layer of mucins for protective purposes.

It is also anticipated that the bowel preparation used prior to sample collection, a necessary procedure to obtain intestinal tissues, could induce certain stress and alter physiological conditions. However, since the regeneration of intestinal epithelium is exceptionally rapid<sup>64</sup> and the stress induced would be equivalent for all the samples, variation in the physiological functions discussed above result largely from the topographical differences of the tissue rather than the bowel preparation. In addition, lipids distribution appeared to be uniform along human intestinal mucosa, which is in contrast to investigations carried out on rats, where enrichment of lipids was observed in jejunum.<sup>29</sup> The major difference between the current and previous investigations was sampling position. Here, human intestinal samples were biopsies, mainly comprising the mucosa part of the intestine, whereas previous work on rats was performed on a cross-sectional biopsy including mucosa, muscle, and peritoneum which could partly contribute to the discrepancy observed.

In conclusion, the biochemical characterization of mucosa along the human GIT including the antrum, duodenum, jejunum, ileum, and transverse colon was achieved from O-PLS-DA data analysis of both the standard 1D and CPMG <sup>1</sup>H HRMAS NMR spectra. The biological composition of the mucosa of human GIT is highly consistent; nevertheless, the variation in patterns of metabolites longitudinally is consistent with local gut function and hence will be of value in assessing disrupted gut mucosal function in pathological tissue samples obtained at biopsies.

**Abbreviations:** CPMG, Carr-Purcell-Meiboom-Gill; GPC, glycerophosphocholine; HRMAS, high-resolution magic-angle spinning; NMR, nuclear magnetic resonance; PE, phosphorylethanolamine; O-PLS-DA, orthogonal projection to latent structure-discriminant analysis; COSY, <sup>1</sup>H-<sup>1</sup>H correlation spectroscopy; TOCSY, <sup>1</sup>H-<sup>1</sup>H total correlation spectroscopy. STOCYS, statistical total correlation spectroscopy; GIT, gastrointestinal tract; PCA, principal component analysis.

**Acknowledgment.** Nestec S.A., Switzerland is acknowledged for the funding of Dr. Y. Wang. H. Tang acknowledges China NSFC (20575074), the Chinese Academy of Sciences (100T program 2005<sup>35</sup>-T12508-O6S138) and National Basic Research Program of China (2006CB503909) for financial supports, and we are grateful to Dr. O. Cloarec for allowing us to use his Matlab scripts for data analysis.

## References

- (1) Schneeman, B. O. *Br. J. Nutr.* **2002**, *88*, S159–S163.

- (2) Dumas, M. E.; Barton, R. H.; Toye, A.; Cloarec, O.; Blancher, C.; Rothwell, A.; Fearnside, J.; Tatoud, R.; Blanc, V.; Lindon, J. C.; Mitchell, S. C.; Holmes, E.; McCarthy, M. I.; Scott, J.; Gauguier, D.; Nicholson, J. K. *Proc. Natl. Acad. Sci. U.S.A.* **2006**, *103*, 12511–12516.
- (3) Bragg, L. E.; Thompson, J. S.; Rikkers, L. F. *Nutrition* **1991**, *7*, 237–243.
- (4) Ferraris, R. P.; Hsiao, J.; Hernandez, R.; Hirayama, B. *Am. J. Physiol.* **1993**, *264*, G285–G293.
- (5) Kiliaan, A. J.; Saunders, P. R.; Bijlsma, P. B.; Berin, M. C.; Taminiau, J. A.; Groot, J. A.; Perdue, M. H. *Am. J. Physiol.: Gastrointest. Liver Physiol.* **1998**, *38*, G1037–G1044.
- (6) Dou, Y. L.; Gregersen, S.; Zhao, J. B.; Zhuang, F. Y.; Gregersen, H. *Dig. Dis. Sci.* **2002**, *47*, 1158–1168.
- (7) Kelly, D.; Campbell, J. I.; King, T. P.; Grant, G.; Jansson, E. A.; Coutts, A. G. P.; Pettersson, S.; Conway, S. *Nat. Immunol.* **2004**, *5*, 104–112.
- (8) Braun-Fahrlander, C.; Riedler, J.; Herz, U.; Eder, W.; Waser, M.; Grize, L.; Maisch, S.; Carr, D.; Gerlach, F.; Bufe, A.; Lauener, R. P.; Schierl, R.; Renz, H.; Nowak, D.; von Mutius, E. *N. Engl. J. Med.* **2002**, *347*, 869–877.
- (9) Hooper, L. V.; Stappenbeck, T. S.; Hong, C. V.; Gordon, J. I. *Nat. Immunol.* **2003**, *4*, 269–273.
- (10) Hooper, L. V.; Gordon, J. I. *Science* **2001**, *292*, 1115–1118.
- (11) Macpherson, A. J.; Gatto, D.; Sainsbury, E.; Harriman, G. R.; Hengartner, H.; Zinkernagel, R. M. *Science* **2000**, *288*, 2222–2226.
- (12) Hooper, L. V.; Midtvedt, T.; Gordon, J. I. *Annu. Rev. Nutr.* **2002**, *22*, 283–307.
- (13) Inagaki, T.; Moschetta, A.; Lee, Y. K.; Peng, L.; Zhao, G. X.; Downes, M.; Yu, R. T.; Shelton, J. M.; Richardson, J. A.; Repa, J. J.; Mangelsdorf, D. J.; Kliewer, S. A. *Proc. Natl. Acad. Sci. U.S.A.* **2006**, *103*, 3920–3925.
- (14) Cheng, L. L.; Lean, C. L.; Bogdanova, A.; Wright, S. C.; Ackerman, J. L.; Brady, T. J.; Garrido, L. *Magn. Reson. Med.* **1996**, *36*, 653–658.
- (15) Wang, Y. L.; Holmes, E.; Nicholson, J. K.; Cloarec, O.; Chollet, J.; Tanner, M.; Singer, B. H.; Utlitzinger, J. *Proc. Natl. Acad. Sci. U.S.A.* **2004**, *101*, 12676–12681.
- (16) Wang, Y. L.; Utzinger, J.; Xiao, S. H.; Xue, J.; Nicholson, J. K.; Tanner, M.; Singer, B. H.; Holmes, E. *Mol. Biochem. Parasitol.* **2006**, *146*, 1–9.
- (17) Marchesi, J. R.; Holmes, E.; Khan, F.; Kochhar, S.; Scanlan, P.; Shanahan, F.; Wilson, I. D.; Wang, Y. L. *J. Proteome Res.* **2007**, *6*, 546–551.
- (18) Brindle, J. T.; Antti, H.; Holmes, E.; Tranter, G.; Nicholson, J. K.; Bethell, H. W. L.; Clarke, S.; Schofield, P. M.; McKilligin, E.; Mosedale, D. E.; Grainger, D. J. *Nat. Med.* **2002**, *8*, 1439–1444.
- (19) Bollard, M. E.; Garrod, S.; Holmes, E.; Lincoln, J. C.; Humpfer, E.; Spraul, M.; Nicholson, J. K. *Magn. Reson. Med.* **2000**, *44*, 201–207.
- (20) Wang, Y.; Bollard, M. E.; Keun, H.; Antti, H.; Beckonert, O.; Ebbels, T. M.; Lindon, J. C.; Holmes, E.; Tang, H.; Nicholson, J. K. *Anal. Biochem.* **2003**, *323*, 26–32.
- (21) Coen, M.; Lenz, E. M.; Nicholson, J. K.; Wilson, I. D.; Pognan, F.; Lindon, J. C. *Chem. Res. Toxicol.* **2003**, *16*, 295–303.
- (22) Bollard, M. E.; Murray, A. J.; Clarke, K.; Nicholson, J. K.; Griffin, J. L. *FEBS Lett.* **2003**, *553*, 73–78.
- (23) Garrod, S.; Humpfer, E.; Spraul, M.; Connor, S. C.; Polley, S.; Connelly, J.; Lindon, J. C.; Nicholson, J. K.; Holmes, E. *Magn. Reson. Med.* **1999**, *41*, 1108–1118.
- (24) Wang, Y. L.; Bollard, M. E.; Nicholson, J. K.; Holmes, E. *J. Pharm. Biomed. Anal.* **2006**, *40*, 375–381.
- (25) Griffin, J. L.; Troke, J.; Walker, L. A.; Shore, R. F.; Lindon, J. C.; Nicholson, J. K. *FEBS Lett.* **2000**, *486*, 225–229.
- (26) Cheng, L. L.; Chang, I. W.; Smith, B. L.; Gonzalez, R. G. *J. Magn. Reson.* **1998**, *135*, 194–202.
- (27) Cheng, L. L.; Wu, C. L.; Smith, M. R.; Gonzalez, R. G. *FEBS Lett.* **2001**, *494*, 112–116.
- (28) Tugnoli, V.; Mucci, A.; Schenetti, L.; Calabrese, C.; Di Febo, G.; Rossi, M. C.; Tosi, M. R. *Int. J. Mol. Med.* **2004**, *14*, 1065–1071.
- (29) Wang, Y. L.; Tang, H. R.; Holmes, E.; Lindon, J. C.; Turini, M. E.; Sprenger, N.; Bergonzelli, G.; Fay, L. B.; Kochhar, S.; Nicholson, J. K. *J. Proteome Res.* **2005**, *4*, 1324–1329.
- (30) Waters, N. J.; Garrod, S.; Farrant, R. D.; Haselden, J. N.; Connor, S. C.; Connelly, J.; Lindon, J. C.; Holmes, E.; Nicholson, J. K. *Anal. Biochem.* **2000**, *282*, 16–23.
- (31) Nicholson, J. K.; Foxall, P. J. D.; Spraul, M.; Farrant, R. D.; Lindon, J. C. *Anal. Chem.* **1995**, *67*, 793–811.
- (32) Meiboom, S.; Gill, D. *Rev. Sci. Instrum.* **1958**, *29*, 688–691.
- (33) Wu, D. H.; Chen, A. D.; Johnson, C. S. *J. Magn. Reson. A* **1995**, *115*, 260–264.

- (34) Hurd, R. E. *J. Magn. Reson.* **1990**, *87*, 422–428.
- (35) Bax, A.; Davis, D. G. *J. Magn. Reson.* **1985**, *65*, 355–360.
- (36) Trygg, J. *J. Chemom.* **2002**, *16*, 283–293.
- (37) Wold, S.; Ruhe, A.; Wold, H.; Dunn, W. J. *SIAM J. Sci. Stat. Comput.* **1984**, *5*, 735–743.
- (38) Wold, S.; Antti, H.; Lindgren, F.; Ohman, J. *Chemom. Intell. Lab. Syst. J.* **1998**, *44*, 175–185.
- (39) Cloarec, O.; Dumas, M. E.; Trygg, J.; Craig, A.; Barton, R. H.; Lindon, J. C.; Nicholson, J. K.; Holmes, E. *Anal. Chem.* **2005**, *77*, 517–526.
- (40) Cloarec, O.; Dumas, M. E.; Craig, A.; Barton, R. H.; Trygg, J.; Hudson, J.; Blancher, C.; Gauguier, D.; Lindon, J. C.; Holmes, E.; Nicholson, J. *Anal. Chem.* **2005**, *77*, 1282–1289.
- (41) Bates, M. D.; Erwin, C. R.; Sanford, L. P.; Wiginton, D.; Bezerra, J. A.; Schatzman, L. C.; Jegga, A. G.; Ley-Ebert, C.; Williams, S. S.; Steinbrecher, K. A.; Warner, B. W.; Cohen, M. B.; Aronow, B. J. *Gastroenterology* **2002**, *122*, 1467–1482.
- (42) Parthasa, S.; Subbaiah, P. V.; Ganguly, J. *Biochemistry* **1974**, *140*, 503–508.
- (43) Labow, B. I.; Souba, W. W. *World J. Surg.* **2000**, *24*, 1503–1513.
- (44) Allen, A. *Trends Biochem. Sci.* **1983**, *8*, 169–173.
- (45) Windmueller, H. G.; Spaeth, A. E. *J. Biol. Chem.* **1980**, *255*, 107–112.
- (46) Budohoski, L.; Challis, R. A. J.; Newsholme, E. A. *Biochem. J.* **1982**, *206*, 169–172.
- (47) Wong, J. M. W.; de Souza, R.; Kendall, C. W. C.; Emam, A.; Jenkins, D. J. A. *J. Clin. Gastroenterol.* **2006**, *40*, 235–243.
- (48) Savage, D. C. *Annu. Rev. Microbiol.* **1977**, *31*, 107–133.
- (49) Xu, J.; Gordon, J. I. *Proc. Natl. Acad. Sci. U.S.A.* **2003**, *100*, 10452–10459.
- (50) Yancey, P. H.; Clark, M. E.; Hand, S. C.; Bowlus, R. D.; Somero, G. N. *Science* **1982**, *217*, 1214–1222.
- (51) Hagihira, H.; Wilson, T. H.; Lin, E. C. *Am. J. Physiol.* **1962**, *203*, 637–640.
- (52) Stevens, B. R.; Wright, E. M. *J. Membr. Biol.* **1985**, *87*, 27–34.
- (53) Kettunen, H.; Peuranen, S.; Tiihonen, K. *Comp. Biochem. Physiol. A Mol. Integr. Physiol.* **2001**, *129*, 595–603.
- (54) Kettunen, H.; Peuranen, S.; Tiihonen, K.; Saarinen, M. *Comp. Biochem. Physiol. A Mol. Integr. Physiol.* **2001**, *128*, 269–278.
- (55) Guan, G. M.; Dai, P. H.; Shechter, I. *Arch. Biochem. Biophys.* **2003**, *417*, 251–259.
- (56) Flogel, U.; Niendorf, T.; Serkova, N.; Brand, A.; Henke, J.; Leibfritz, D. *Neurochem. Res.* **1995**, *20*, 793–802.
- (57) Hagen, T. M.; Wierzbicka, G. T.; Bowman, B. B.; Aw, T. Y.; Jones, D. P. *Am. J. Physiol.* **1990**, *259*, G530–G535.
- (58) Loguercio, C.; Romano, M.; Disapio, M.; Nardi, G.; Taranto, D.; Grella, A.; Blanco, C. D. *Scand. J. Gastroenterol.* **1991**, *26*, 1042–1048.
- (59) Hoensch, H.; Morgenstern, I.; Petereit, G.; Siepmann, M.; Peters, W. H. M.; Roelofs, H. M. J.; Kirch, W. *Gut* **2002**, *50*, 235–240.
- (60) Loguercio, C.; Di Pierro, M. *Ital. J. Gastroenterol. Hepatol.* **1999**, *31*, 401–407.
- (61) Portela-Gomes, G. M.; Stridsberg, M.; Johansson, H.; Grimelius, L. *Histochem. Cell Biol.* **1999**, *111*, 49–54.
- (62) Strous, G. J.; Dekker, J. *Crit. Rev. Biochem. Mol. Biol.* **1992**, *27*, 57–92.
- (63) Allen, A.; Flemstrom, G.; Garner, A.; Kivilaakso, E. *Physiol. Rev.* **1993**, *73*, 823–857.
- (64) Potten, C. S. *Philos. Trans. R. Soc. London, Ser. B: Biol. Sci.* **1998**, *353*, 821–830.

PR0702565